Hindawi
International Journal of Antennas and Propagation
Volume 2021, Article ID 9218255, 12 pages
https://doi.org/10.1155/2021/9218255

Research Article

A Low-Profile Dual-Polarized MIMO Antenna with an AMC Surface for WLAN Applications

Xinghui Jin, Yang Qiu, Di Wu, Guoliang Yu, Rongdi Guo, Guohua Wu, Mingmin Zhu, and Hao-Miao Zhou

Key Laboratory of Electromagnetic Wave Information Technology and Metrology of Zhejiang Province, College of Information Engineering, China Jiliang University, Hangzhou 310018, China

Correspondence should be addressed to Mingmin Zhu; mzhu@cjlu.edu.cn and Hao-Miao Zhou; zhouhm@cjlu.edu.cn

Received 20 April 2021; Revised 10 August 2021; Accepted 14 September 2021; Published 20 October 2021

Academic Editor: Claudio Gennarelli

In this paper, a low-profile dual-polarized MIMO antenna with an artificial magnetic conductor (AMC) for WLAN applications is proposed. The antenna consists of two Barron structured feeds combined with each other in ±45° polarization. The significant low-profile ($0.098\lambda_0$) advantage of this antenna is achieved by loading an AMC reflector on the bottom of the antenna. The AMC reflector is composed of a patch of 4×4 units, which enables the low profile and high gain of the antenna. The antenna is simulated, processed, and measured physically, and the measured results show that the proposed dual-polarized antenna has a bandwidth of 21% (2.35–2.89 GHz), a peak gain of 7.34 dBi, and a peak efficiency of 71.5%, which can be used for applications such as WLAN base station antennas.

1. Introduction

With the rapid development of wireless communication, the requirement of base station antenna is increasing. To save antenna installation space, reduce wind resistance, and improve stability, the base station antenna requires a lower profile. At the same time, in order to reduce the radiation energy scattering cross section of the base station antenna and achieve efficient signal transmission, the base station antenna usually needs to achieve unidirectional radiation pattern [1]. Therefore, low-profile unidirectional radiation antennas are widely used in communication base stations and some other fields such as autopilot vehicles and spacecraft. Loading AMC electromagnetic surfaces with high impedance and in-phase reflection characteristics is an effective method to achieve low-profile and unidirectional radiation in antenna design. Furthermore, to make full use of the limited spectrum resources and advance the transmission speed and quality of electromagnetic signals, dual-polarized antenna, especially ±45° polarized antenna, is a useful antenna type to solve the multipath fading problem, reducing the number and cost of antennas [2].

The conventional antenna needs to be placed at 1/4 times the wavelength of the radiated electromagnetic wave above the ground surface to achieve the effect of unidirectional radiation pattern. In the existing works, such as [3–5], broadband dual-polarized antennas using metallic reflective surfaces with stable directional radiation patterns were proposed, but the profile height of the antenna is greater than 1/4 wavelength. The higher the profile height of the antenna is, the more detrimental it is to the development of antenna miniaturization. Therefore, it is necessary to find a new reflection structure to reduce the profile of the antenna. Researchers have found that manufactured electromagnetic metamaterial have electromagnetic properties that natural materials do not have, such as negative permeability, negative dielectric constant, and so on. These electromagnetic characteristics can be used to adjust the phase, amplitude, and propagation direction of electromagnetic wave [6]. AMC is one of the electromagnetic metamaterials. When a plane wave is incident on an AMC structure, the phase difference between the reflected wave and the incident wave at this frequency is zero, and the profile height of the antenna can break 1/4 times the wavelength boundary. Therefore,

AMC conductors are widely used in unidirectional radiation antennas, especially for low-profile antenna design and enhancing unidirectional radiation [7–9]. For example, Li et al. [10] presented a miniaturized AMC reflector with a reflection phase of 5–8 GHz (45.45%) which can reduce the undesired backside radiations by 20 dB more efficiently compared with conventional PEC (perfect electric conductor) structures. In [11], a multilayer artificial magnetic conductor surface was used, which clearly increases the complexity and cost of antenna fabrication and is not utilized for large-scale antenna applications. Sarkar and Gupta [12] designed a dual-band circularly polarized antenna for RFID readers using an artificial magnetic conductor, which achieves dual band by etching slits in the patch but only has bandwidths of 5.25% and 2%. Lee et al. [13] designed a low-profile dual-polarized antenna containing a metal cube. The antenna size was reduced by using a dielectric substrate. However, the antenna has limited efficiency which is not more than 50%. By introducing a novel AMC meta-surface structure into the dielectric resonator antenna, Khan et al. [14] successfully reduced the size of the antenna by 85%. Son Xuat Ta and Ikmo Park [15] creatively proposed a T-shaped slits AMC structure and reduced the reflection phase from 2.65 GHz to 2.35 GHz, which also makes the antenna miniaturized. It is worth mentioning that the antennas in [14, 15] have very high gain and efficiency of over 70%. Ameen et al. and Volkov et al. [16, 17] proposed that AMC structures can be applied to the design of broadband satellite antennas and synthetic aperture radar (SAR) with bandwidth ranging from 2.23 to 2.91 GHz (26.45%) and 1.6 to 2.4 GHz (40%). Although a large amount of related work has been proposed, how to design a low-profile dual-band dual-polarized MIMO antenna with good performance is still one of the hot research topics.

In this paper, a dual-polarized low-profile MIMO antenna with an AMC surface operating in 2.6 GHz is proposed. The proposed antenna consists of a three-layer structure: the bottom layer is a thin dielectric substrate with feed lines to provide excitation for the antenna, the middle is an AMC structure that enables the antenna to achieve low-profile and unidirectional radiation, and the upper layer is the antenna, which is connected to the feed lines at the front and the ground at the back. The antenna structure is simulated and fabricated. Experimental tests are carried out, and the measured results show that the proposed antenna has a good practical value.

2. Antenna Design

2.1. Design Evolution of Basic Radiation Antennas. Monopole antenna is a common microstrip antenna structure that can generate more omnidirectional radiation, but its gain is not high, and its impedance bandwidth is relatively narrow, which cannot meet the actual requirements of antenna's unidirectional radiation. The unidirectional radiation performance of the monopole antenna can be achieved by using the AMC meta-surface structure. Usually, an AMC unidirectional radiation antenna consists of a basic radiation antenna and an AMC reflection structure. In order to simplify the design of radiation antenna, the U-shaped monopole antenna is selected as the basic antenna, as shown in Figure 1(a). The top layer of substrate is a long U-shaped bent microstrip line (blue part of the schematic), which changes the current flow path by folding to reduce the actual electric length of the antenna. Barron structure is used to improve the impedance matching of antennas and broaden the bandwidth. In order to further fine-tune the center frequency and bandwidth of AMC, a rectangular slot is opened on each side of the rectangular patch unit. The surface impedance and reflection phase can be effectively changed by adjusting the size of the slot. The simulation results of Ant. 1 is shown in Figure 2(a). The operating band is 2.51–3.70 GHz, and the bandwidth is 1190 MHz, which shows that the antenna has good impedance matching.

In fact, the electromagnetic signal of a single antenna can be transmitted inefficiently because of external interference, so it needs multiple antennas to transmit the electromagnetic signal jointly and keep the coupling between antennas at a low level by means of dual polarization. Ant. 1 alone is not enough to achieve this, so the U-shaped structure in Ant. 1 needs to be improved. Without changing the antenna radiation performance, two antenna radiation structures need to be assembled in order to achieve dual polarization of the antenna. Therefore, the antenna structure is optimized as shown in Figures 1(b) and 1(c). On the basis of Ant. 1, Ant. 2, shown in Figure 1(b), bends the U-type microstrip line slightly upwards and slots the lower side and Ant. 3, shown in Figure 1(c), bends the microstrip line slightly downward, and the substrate is slotted on the lower side. The results of Ant. 2 and Ant. 3 simulation *S*-parameters are plotted in Figure 2(a). From the chart, it can be seen that the results of Ant. 2 and Ant. 3 are basically in agreement with Ant. 1, indicating that bending and slotting have little influence on antenna performance and can be ignored.

Finally, Ant. 2 and Ant. 3 are cross assembled into the final dual-polarization antenna radiation structure, Ant. 4, as shown in Figure 1(d). The lower part of the two antennas is used to load AMC reflection structure. From the pattern in Figure 1(a), it can be seen that the two L-shaped grounding structures at the bottom of the substrate make the far-field radiation of the antenna perpendicular to the substrate. Therefore, crossing the two antennas can give the two antennas very low mutual radiation interference. Furthermore, the grounding part of the antenna is in the same position as the grounding surface of the AMC, which facilitates AMC placement and port feeding. The *S*-parameters of Ant. 4 are simulated. As shown in Figure 2(b), the operating frequency band of the antenna is 2.50–3.70 GHz. Compared with the results of Ant. 1, the deviation is only 10 MHz, and the isolation between the two ports of Ant. 4 is greater than 22 dB. The antenna has a good overall performance.

2.2. Analysis of the AMC Unit Cell. The reflective structure is composed of several AMC units, each consisting of a metal ground, a patch, and a dielectric substrate. The most conventional reflective structure is the PEC, which is a metal

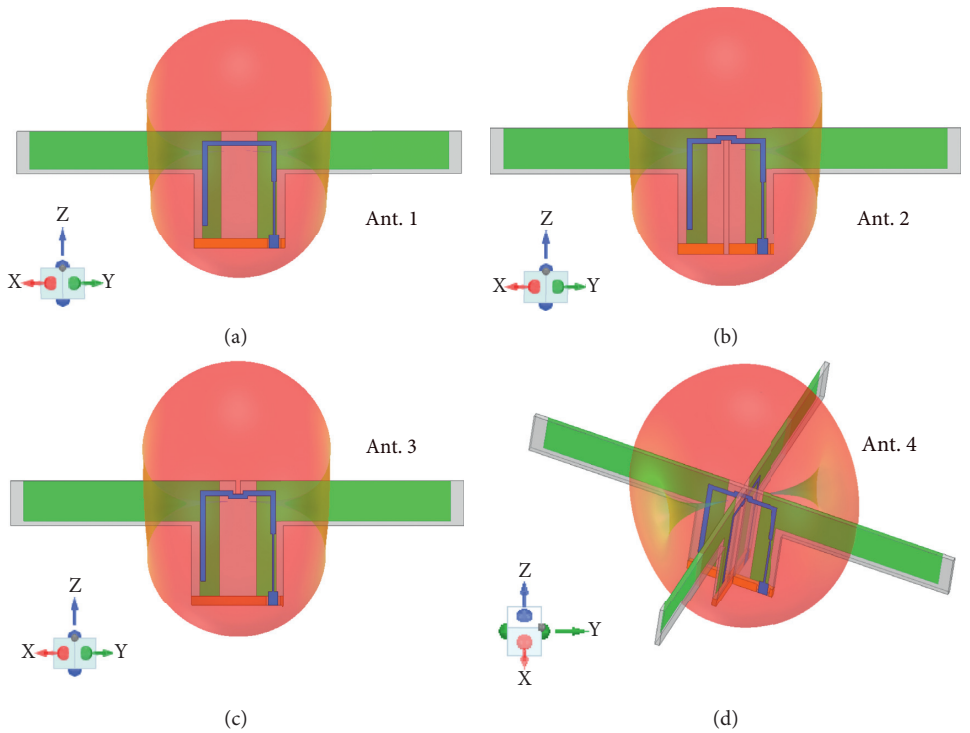

Figure 1: Antenna configuration evolution.

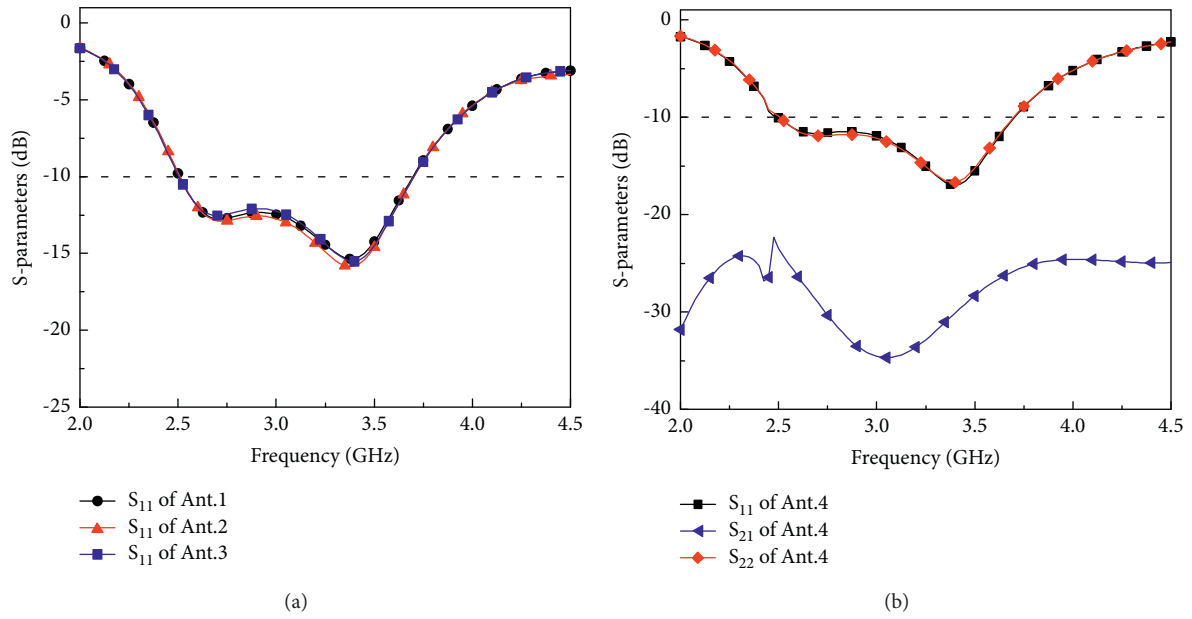

Figure 2: Simulated *S*-parameters of the radiating element evolution.

patch covering the entire dielectric substrate. It is well known that when an incident wave passes through a PEC structure, the phase of the reflected wave will change 180 degrees. However, there is an electromagnetic band gap in AMC, which can realize in-phase reflection of waves, so we choose AMC as the reflection structure. The operating frequency band and surface impedance can be adjusted by changing the size of the reflector patch. Referring to PEC rectangular patch, we change the size of the rectangular patch to reserve a certain distance (2.5 mm) between the patch and the substrate, so as to form a band gap and realize AMC reflection unit. The optimum analysis of the size parameter selection is given below. On the bottom of the substrate, there are two L-shaped metal patches (green part

of the schematic) as the ground. And a metal strip (orange part of the schematic) below the antenna is used to feed the microstrip line. The final AMC cell structure is shown in Figure 3(a).

The antenna geometry, as shown in Figure 1, consists of a square patch with an edge length of $L2$ and four rectangular slots with a length of $L3$ and a width of $W1$. The 0° reflection phase point and reflection bandwidth of AMC can be adjusted by changing the shape and size of patch and slot. The patch material is copper and is printed on a FR4 substrate with a thickness of $h1$ and an edge length of $L1$. It is well known that AMC can be used to improve the gain and reduce the profile of the antenna. The resonant frequency of the AMC surface corresponds to 0° of the reflection phase, and the reflection bandwidth is defined as the frequency range from −90° to 90° of the reflection phase. In order to obtain the optimal AMC reflection structure, the above structure parameters are optimized and simulated. Figure 3(c) shows the reflection phase when the thickness of the dielectric substrate $h1$ is changed. It can be seen from the figure that when $h1$ is 1 mm, 3 mm, 5 mm, and 10 mm, respectively, the reflection bandwidth of AMC is shifting to the low frequency, and the bandwidth is increasing, which indicates that the operating frequency of AMC can be reduced and the operating bandwidth can be widened by increasing the thickness of the substrate.

The simulated reflection phase curves of the AMC unit for different parameter sizes can be observed in Figure 4. In Figure 4(a), the values of $L1$ are 26 mm, 28 mm, and 30 mm, respectively, and the center frequency shifts slightly toward the high frequency when $L1$ increases. Figure 4(b) shows that the size of $L2$ has a great influence on the center frequency and bandwidth. When $L2$ values are 19 mm, 21 mm, 23 mm, and 25 mm respectively, the center frequency shifts to low frequency and the bandwidth becomes narrow. The overall effect of different values of $L3$ and $W1$ on the performance of the AMC cell is not significant and can be used to fine-tune the reflected phase of the AMC, as shown in Figures 4(c) and 4(d).

After extensive simulations, the selected patch sizes are as follows: $h1 = 5$ mm, $L1 = 28$ mm, $L2 = 23$ mm, $L3 = 6$ mm, and $W1 = 2.5$ mm. The AMC unit cells operate in the band of 2.38–2.68 GHz. It is worth noting that the AMC surface proposed in this paper is chosen as 4×4 units. The simulation results of loading the AMC surface with different cells are shown in Figure 5. When the AMC surface is chosen as 2×2 units, the peak gain and peak efficiency of the antenna are 6.05 dBi and 81.5%, respectively. When 4×4 cells are loaded, the corresponding peak gain and efficiency are 6.88 dBi and 77.7%, and the efficiency decreases by 3.8%, but the gain increases by 0.83 dBi. When 6×6 cells are loaded, the peak gain and efficiency are 5.58 dBi and 72.7%, and the gain and efficiency are both reduced. When 8×8 cells are selected, the gain and efficiency continue to decrease. Figure 5(b) shows the simulated results of the antenna radiation patterns. Considering the overall size and operating performance of the antenna, 4×4 units are selected as the antenna reflector.

3. Simulated and Measured Results

3.1. Antenna Configuration. According to the analysis and evolution of the above basic antenna and AMC reflection structure, a dual-polarization MIMO antenna with AMC reflection structure can be given, as shown in Figure 6. The antenna configuration consists of an AMC structure with $h1$ thickness and FR4 substrate with $h2$ and two antennas. The material used for both the AMC substrate and the antenna substrate is FR4 with the relative permittivity of 4.4 and the dielectric loss tangent of 0.02. Figure 6(a) shows the top view of the antenna, and it can be seen that 16 AMC units form a 4×4 AMC reflector with side length L. Above the AMC reflector, two antennas are inserted crosswise into the holes and fixed directly on the AMC substrate without adding additional support. The antenna height above the AMC surface is $h3$. The AMC surface is on the upper surface of the substrate for in-phase reflection. The middle of the two layers is ground which ensures total reflection of the electromagnetic wave energy. The antenna is a dual-port MIMO antenna. Each of the two ports excites one antenna, and the two excitation ports are on the side of the bottom board. The excitation port is connected to the feed line on the bottom side, and the two feed lines are placed on the bottom side to avoid contact with the ground. By the reflection characteristics of AMC, the profile height of the antenna is reduced to H, about $0.098\lambda_0$, which is much smaller than the theoretical $0.25\lambda_0$, as shown in Figure 6(b).

The schematic diagram of the two antennas is presented in Figures 6(c) and 6(d). The antenna consists of a substrate with a thickness of $h2$ and two symmetric L-type structures with dimensions of $L4 \times h4$ and $L5 \times h8$. The "L" shape allows the antenna to have wide possible range of radiation. The two antennas are notched so that these can be cross-mounted together. The front and back of the antennas are printed with radiation patches to increase the radiation strength. The bottom of the antenna is plated with copper, which acts as a conductor when the two antennas are mounted together. The antenna structure is obtained by simulated design, and its detailed dimensions are given in Table 1.

3.2. Results and Discussion of the Proposed Antenna. The physical antenna was fabricated, as shown in Figure 7. The antenna's S-parameter performance was measured using the Agilent N5230C vector network analyzer, and the radiation properties including efficiency, gain, and radiation patterns were measured in a SATIMO microwave anechoic chamber. The simulated and measured S-parameters, gain, and efficiency are given in Figures 8 and 9. The comparison in the figures shows that the simulated and measured results are in good agreement, but there are slight differences, which are due to the effects of processing, soldering, and other equipment errors. Figure 8 shows the reflection coefficients for two ports, and it can be seen that the operating band is 2.34–2.89 GHz for the simulation and 2.35–2.89 GHz for the test, with a relative bandwidth of 21%. In the operating band range, the simulated isolation reaches 22 dB and the

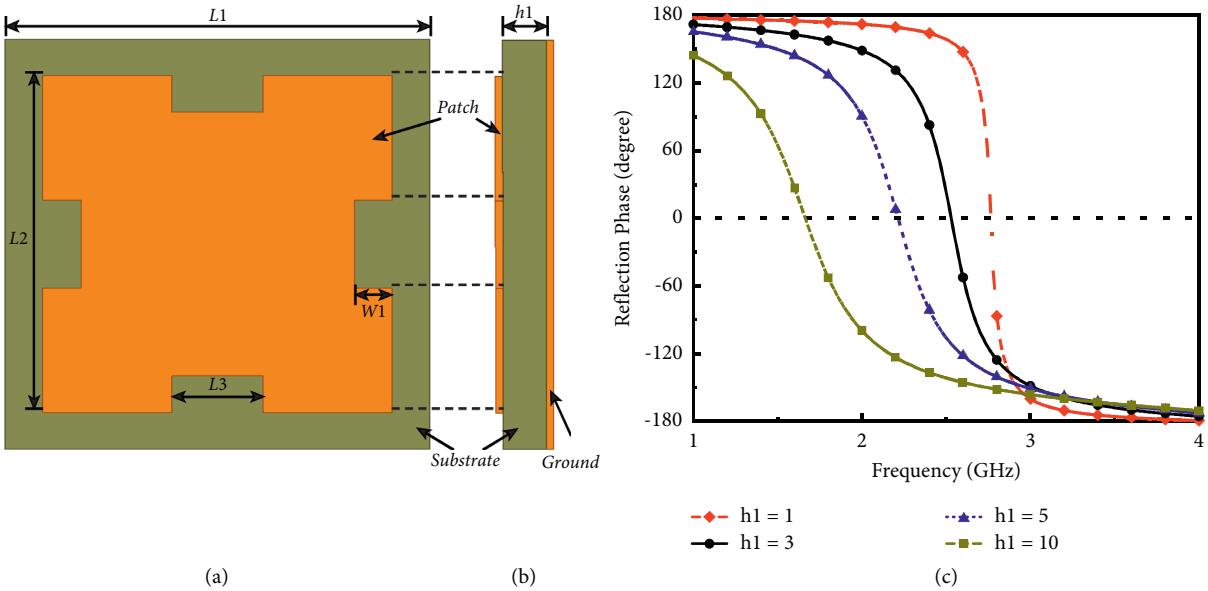

Figure 3: Dimensions of the AMC: (a) top view; (b) side view; (c) reflection phases of varying $h1$.

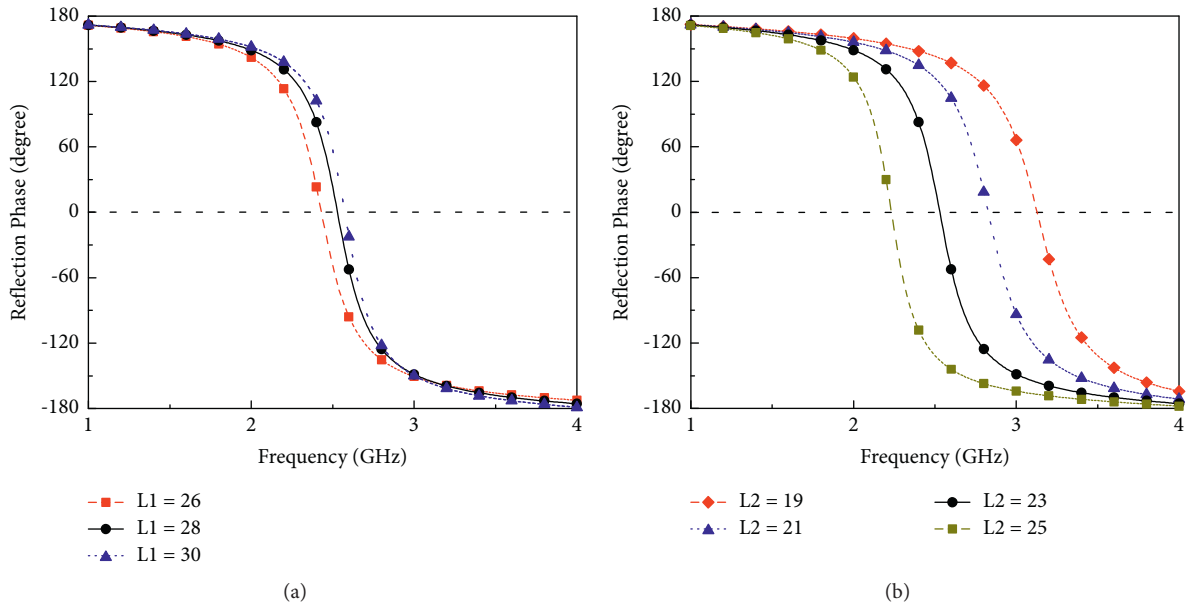

Figure 4: Continued.

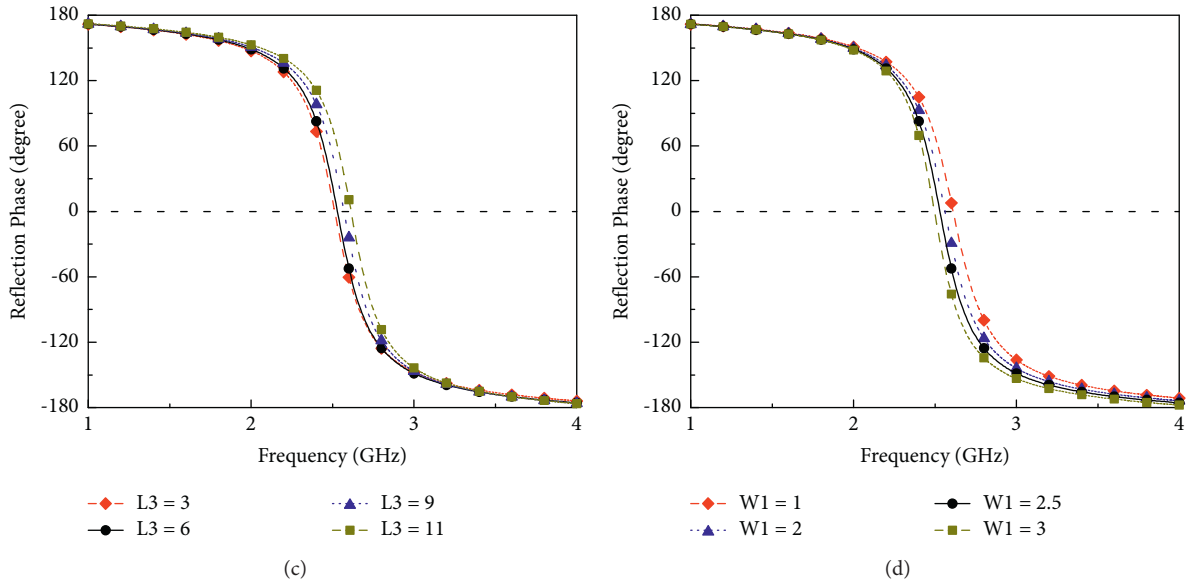

Figure 4: Simulated reflection phases: (a) varying $L1$; (b) varying $L2$; (c) varying $L3$; (d) varying $W1$.

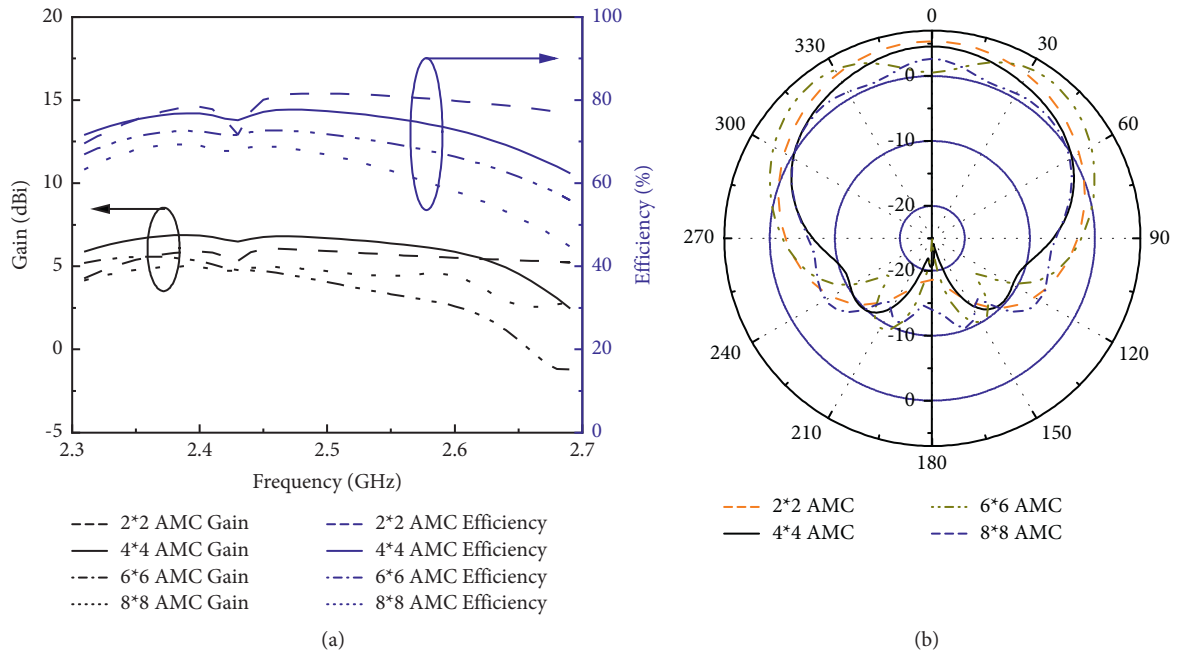

Figure 5: Simulated results of various AMC surfaces: (a) gain and efficiency; (b) radiation patterns.

measured isolation reaches 19 dB. It can also be observed from Figure 7(b) that the simulated gain of the antenna in the band range of 2.28–2.59 GHz is greater than 5 dBi with a peak gain of 6.8 dBi, and the simulated efficiency in the band range of 2.29–2.63 GHz is greater than 70%. The measured results are better than the simulated results with gain greater than 5 dBi and peak gain of 7.34 dBi in the band range of 2.3–2.65 GHz, and the efficiency is greater than 60% in the range of 2.4 GHz–2.7 GHz with peak efficiency up to 71.5%, which still has good efficiency. In Figure 9(b), the efficiency of AMC structure without adding AMC is shown to be more than 90%. After adding AMC structure, the efficiency decreases to some extent. This is because the AMC has a high impedance and part of the energy of the port is lost on the AMC, resulting in lower energy radiation from the antenna. At the same time, it can be seen from the figure that the gain of the antenna on the operating frequency band of reflective structure AMC is much higher than that of the basic antenna without AMC. The effect of gain improvement brought by efficiency reduction is very significant, and the result is better than the simulation result, and the unidirectional radiation of AMC structure to the electromagnetic wave is realized.

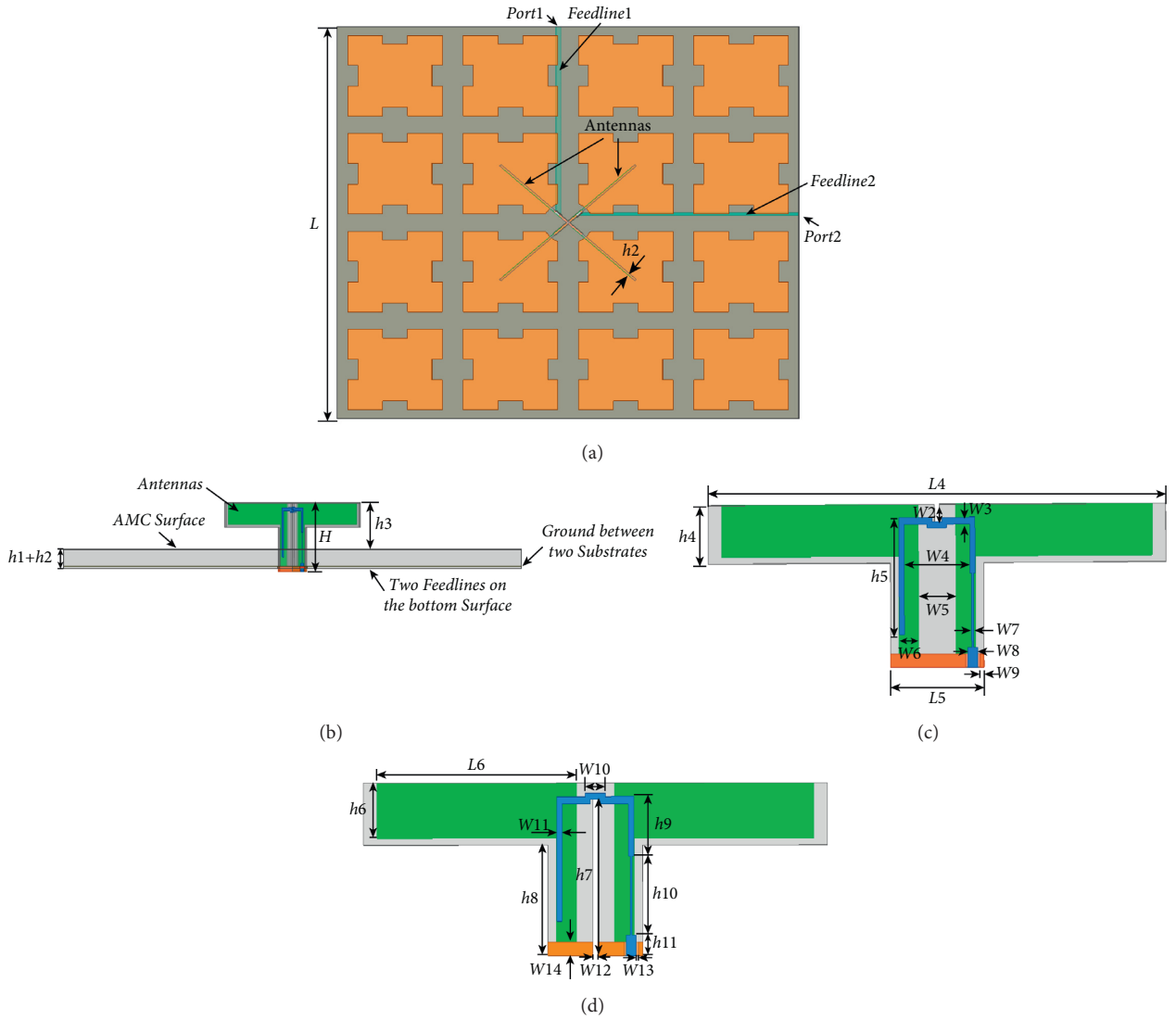

Figure 6: Geometry of the proposed antenna: (a) top view; (b) side view; (c) antenna element 1; (d) antenna element 2.

Table 1: Design parameters of the proposed antenna.

Parameter	Value (mm)
L	112
$L3$	6
$L6$	20
$W3$	0.52
$W6$	2
$W9$	0.45
$W12$	0.55
$h1$	3
$h4$	4.5
$h7$	11.3
$h10$	5.7
$L1$	28
$L4$	46.5
$W1$	2.5
$W4$	6.68
$W7$	0.2
$W10$	2

Table 1: Continued.

Parameter	Value (mm)
$W13$	0.2
$h2$	0.5
$h5$	9
$h8$	8
$h11$	1.5
$L2$	23
$L5$	9.5
$W2$	1.33
$W5$	3.8
$W8$	1
$W11$	0.52
$W14$	1
$h3$	8.5
$h6$	4
$h9$	4.3
H	12.5

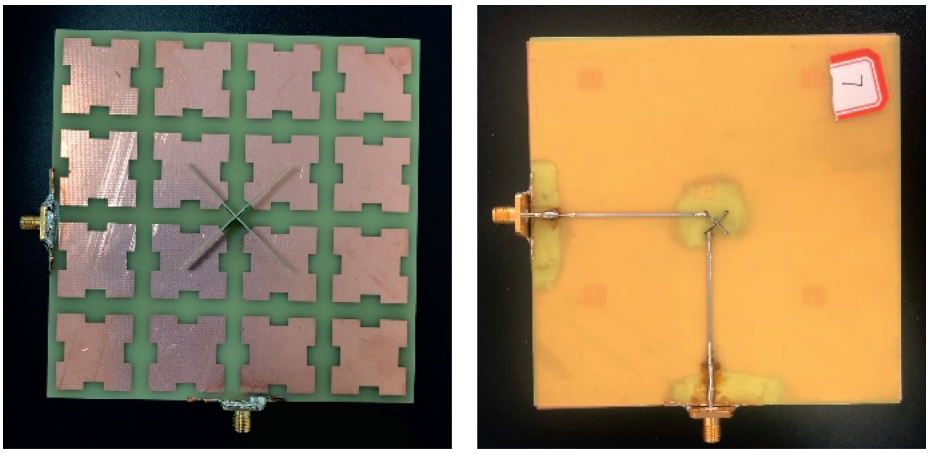

(a) (b)

Figure 7: Photograph of the proposed antenna in (a) top view and (b) bottom view.

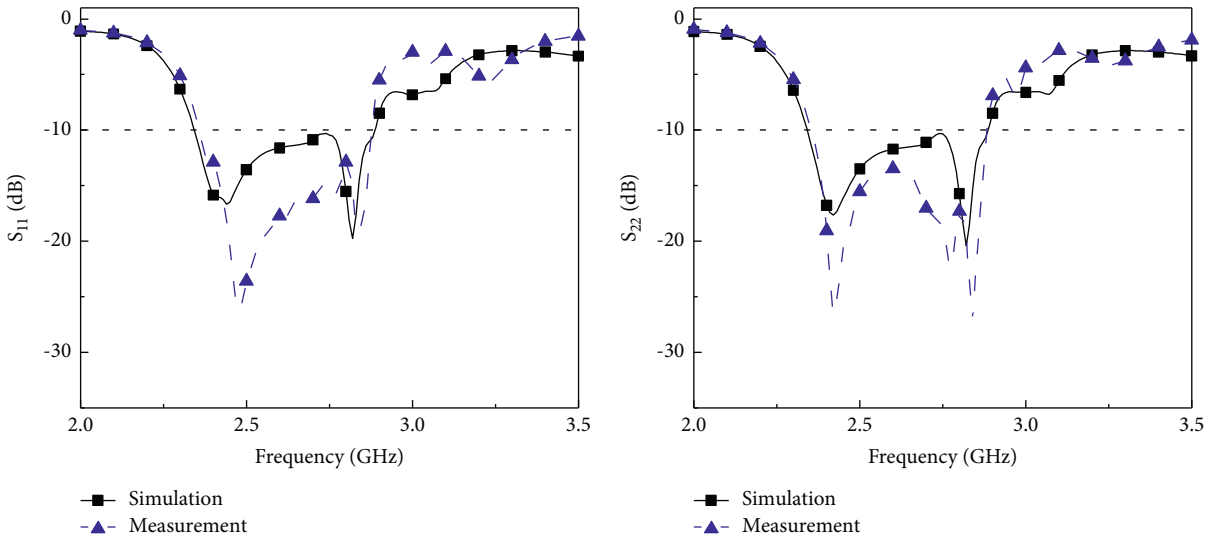

(a) (b)

Figure 8: Simulated and measured S-parameters of (a) port 1 and (b) port 2.

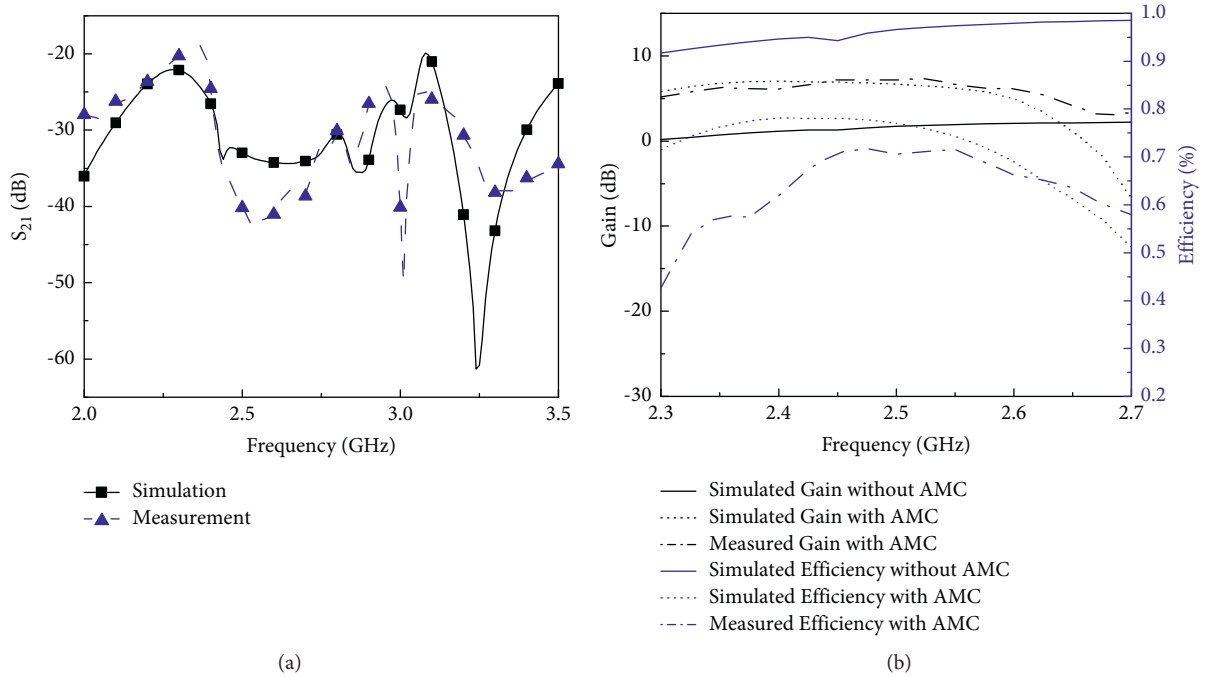

FIGURE 9: Simulated and measured results of (a) S_{21} and (b) gain and efficiency.

The simulated and measured radiation patterns of the proposed antenna at 2.43 GHz, 2.65 GHz, and 2.84 GHz are displayed in Figure 10. Since the antenna is symmetric, only the radiation patterns when port 1 is excited are given. As can be seen from the figure, at 2.43 GHz, 2.65 GHz, and 2.84 GHz, the antenna has cross polarization of about 10 dB, 20 dB, and 25 dB, respectively, which makes the antenna have better radiation in the main polarization direction. In general, within the required operating frequency band, the antenna has good radiation intensity and polarization, showing a dual-polarization directional radiation state. It can be discovered that the simulated and measured results are basically the same, and the differences are mainly caused by the limited accuracy of the measurements and the errors in fabrication and assembly.

Figure 11 shows the radiation patterns of the proposed antenna at 2.43 GHz, 2.65 GHz, and 2.84 GHz. The simulated radiation patterns of the basic antenna without AMC structure are shown in Figure 11(a). The radiation of the antenna is mainly along the positive and negative directions of the z-axis. The measured radiation patterns of the antenna on the three coordinate axis planes with AMC surface are shown in Figure 11(b). It can be seen from the figure that in the x-y plane, the radiation intensity in the directions of 30° and 210° is strong, and the overall radiation patterns are approximately circular. In the x-z and y-z planes, the radiation intensity in the $+z$-axis direction is much better than that in the $-z$-axis direction. This shows that the antenna presents good unidirectional radiation under the action of AMC structure. However, since the operating bandwidth range of the basic antenna is wider than the reflection bandwidth range of AMC, the radiation effect of the antenna at $+z$-axis at 2.84 GHz is not as good as 2.43 GHz and 2.65 GHz.

The proposed antenna is compared with the existing antennas in Table 2. As can be seen from Table 2, the biggest advantage of the antenna proposed in this paper is that the total height of the antenna is only 12.5 mm, and the profile height is only $0.098\lambda_0$. The occupancy rate of space is greatly reduced. Compared with other antennas in Table 2, the antenna proposed in this paper is obviously superior to all other antennas except reference [2] in size and profile height. Compared with reference [2], the size and profile height of the antenna proposed in this paper are slightly larger than that in reference [2], but the bandwidth, gain, and efficiency of the antenna are better than those in reference [2]. Secondly, the relative bandwidth of this antenna is 21%, which is obviously better than other antennas except reference [16], the gain is better than the results of references [2, 16], and the efficiency is better than the results of references [2, 13]. Therefore, considering the overall effect of the proposed antenna in terms of profile height, coverage bandwidth, gain,

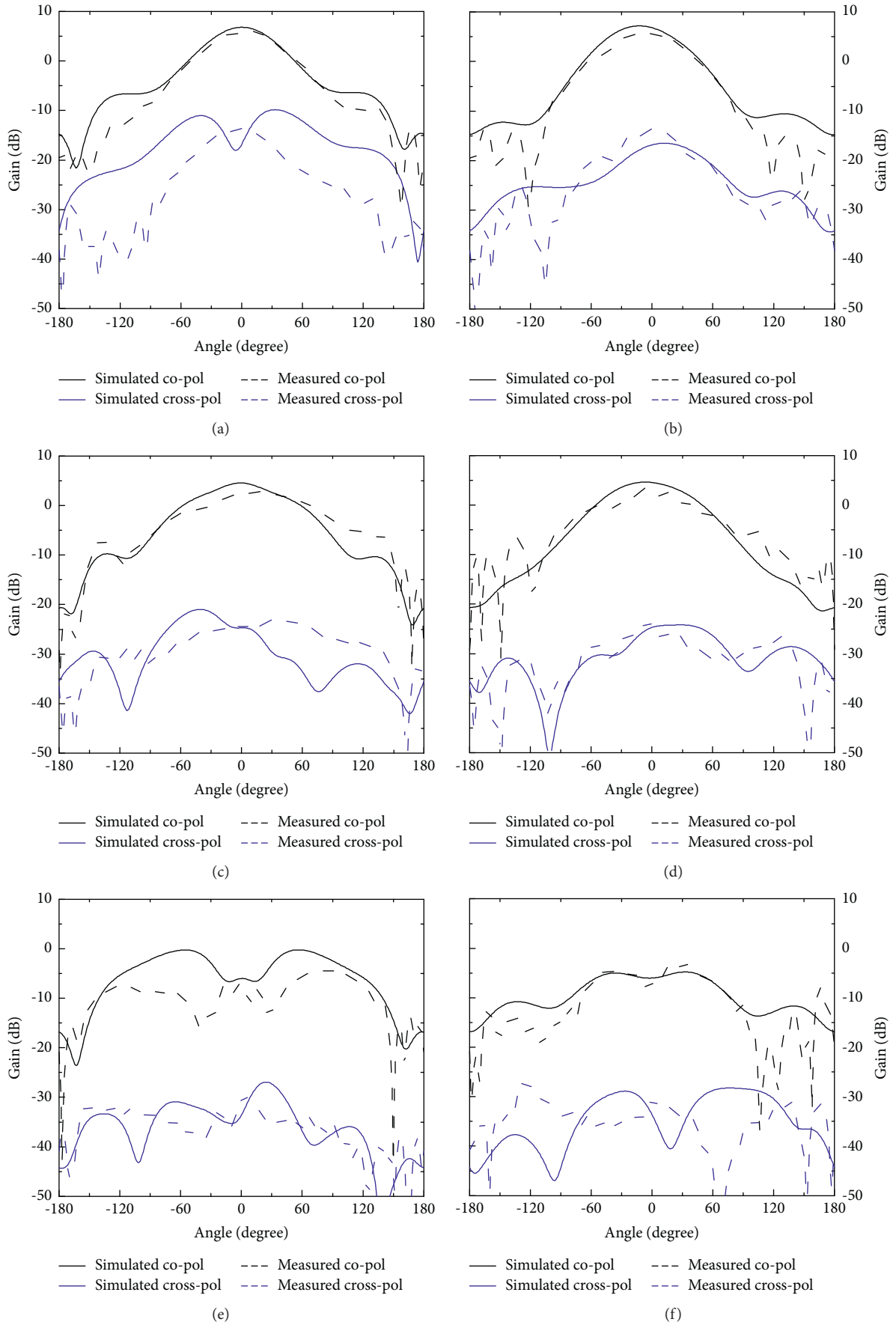

Figure 10: Simulated and measured polarization patterns of the proposed antenna. (a) E-plane at 2.43 GHz. (b) H-plane at 2.43 GHz. (c) E-plane at 2.65 GHz. (d) H-plane at 2.65 GHz. (e) E-plane at 2.84 GHz. (f) H-plane at 2.84 GHz.

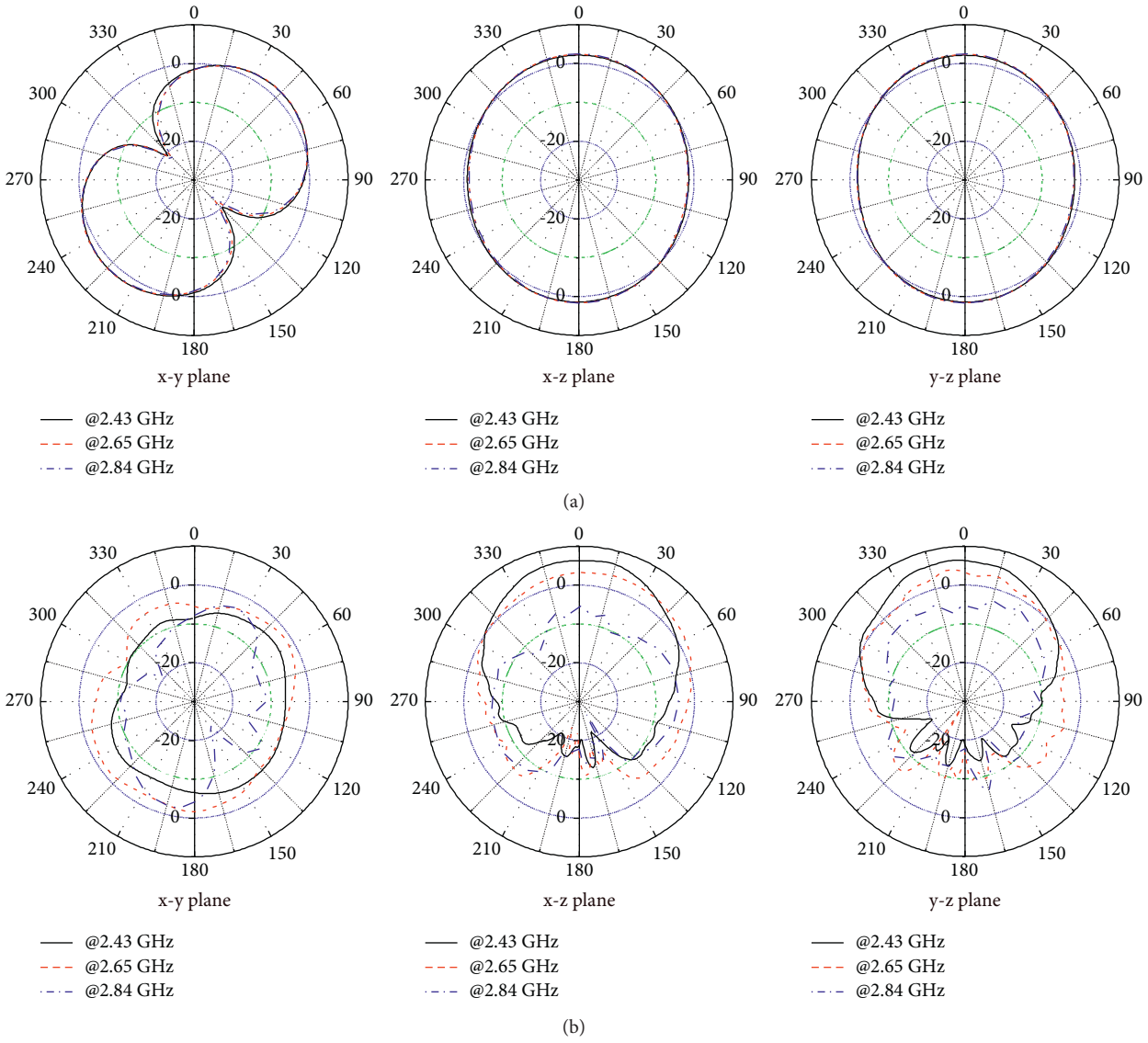

Figure 11: (a) Simulated radiation patterns of basic antenna without AMC at 2.43 GHz, 2.65 GHz, and 2.84 GHz. (b) Measured radiation patterns of basic antenna with AMC at 2.43 GHz, 2.65 GHz, and 2.84 GHz.

Table 2: Comparison of proposed antenna with existing works.

Ref.	Size (lambda^3)	Bandwidth (GHz)	Isolation (dB)	Gain (dBi)	Efficiency	Polarization
[1]	$0.91 \times 0.91 \times 0.26$	7.7% (2.5–2.7) 8.7% (3.3–3.6)	≥25	8.4	N/A	Dual
[2]	$0.87 \times 0.87 \times 0.09$	15.6% (2.36–2.76) 9.3% (5.12–5.62)	≥22	7.3	65%	Dual
[7]	$1.01 \times 1.01 \times 0.13$	18.6% (2.28–2.75)	≥30	N/A	N/A	Dual
[13]	$0.62 \times 0.62 \times 0.12$	16.5% (2.4–2.83)	≥35	9.6	45%	Dual
[16]	$0.72 \times 0.72 \times 0.16$	26.5% (2.23–2.91)	≥14.5	7.02	N/A	CP
[18]	$0.93 \times 0.93 \times 0.13$	19.8% (3.14–3.83) 13.2% (4.40–5.02)	≥20	8.2	90%	Dual
This work	$0.91 \times 0.91 \times 0.10$	21% (2.35–2.89)	≥19	7.34	71.5%	Dual

and efficiency, compared with the existing antennas, it has better electromagnetic characteristics and can meet the requirements of wireless communication system.

4. Conclusion

In this paper, a low-profile dual-polarized MIMO antenna loaded with AMC surface is proposed. The profile of the antenna is reduced to $0.098\lambda_0$ with the AMC surface loaded. The antenna operates at the band of 2.35 GHz–2.89 GHz, and the peak gain and peak efficiency are measured to be 7.34 dBi and 71.5%, respectively. The simulation and test results are in general agreement. The results show that the proposed antenna has good performance and is suitable for multiple applications such as WLAN for base stations, LTE2500, Bluetooth, and 5G for China Mobile.

Data Availability

The data used to support the findings of this study are available from the corresponding author upon request.

Conflicts of Interest

The authors declare that they have no conflicts of interest.

Authors' Contributions

Xinghui Jin and Yang Qiu contributed equally to this study.

Acknowledgments

This study was supported by the Funds of the National Natural Science Foundation of China under grant nos. 11972333, 11902316, and 51902300 and the Natural Science Foundation of Zhejiang Province under grant nos. LZ19A020001, LQ19F010005, and LY21F010011. The antenna's efficiency, gain, and pattern were measured in Hangzhou RFID Center-CAS. The authors would like to express their sincere appreciation for the support.

References

[1] Y. Liu, S. Wang, N. Li, J.-B. Wang, and J. Zhao, "A compact dual-band dual-polarized antenna with filtering structures for sub-6 GHz base station applications," *IEEE Antennas and Wireless Propagation Letters*, vol. 17, no. 10, pp. 1764–1768, 2018.

[2] H. Zhai, K. Zhang, S. Yang, and D. Feng, "A low-profile dual-band dual-polarized antenna with an AMC surface for WLAN applications," *IEEE Antennas and Wireless Propagation Letters*, vol. 16, pp. 2692–2695, 2017.

[3] Q.-X. Chu, D.-L. Wen, and Y. Luo, "A broadband ±45° dual-polarized antenna with Y-shaped feeding lines," *IEEE Transactions on Antennas and Propagation*, vol. 63, no. 2, pp. 483–490, 2015.

[4] R. Wu and Q.-X. Chu, "A wideband dual-polarized antenna for LTE700/GSM850/GSM900 applications," *IEEE Antennas and Wireless Propagation Letters*, vol. 16, pp. 2098–2101, 2017.

[5] L.-H. Wen, S. Gao, C.-X. Mao et al., "A wideband dual-polarized antenna using shorted dipoles," *IEEE Access*, vol. 6, pp. 39725–39733, 2018.

[6] V. G. Veselago, "The electrodynamics of substances with simultaneously negative values of ϵ and μ," *Soviet Physics-Uspekhi*, vol. 10, no. 4, pp. 509–514, 1968.

[7] B. Li, W. Hu, J. Ren, and Y.-z. Yin, "Low-profile dual-polarized patch antenna with HIS reflector for base station application," *Journal of Electromagnetic Waves and Applications*, vol. 28, no. 8, pp. 956–962, 2014.

[8] Z. Nie, H. Zhai, L. Liu, J. Li, D. Hu, and J. Shi, "A dual-polarized frequency-reconfigurable low-profile Antenna with harmonic suppression for 5G application," *IEEE Antennas and Wireless Propagation Letters*, vol. 18, no. 6, pp. 1228–1232, 2019.

[9] J. Liu, J.-Y. Li, J.-J. Yang, Y.-X. Qi, and R. Xu, "AMC-loaded low-profile circularly polarized reconfigurable antenna array," *IEEE Antennas and Wireless Propagation Letters*, vol. 19, no. 7, pp. 1276–1280, 2020.

[10] G. Li, H. Zhai, L. Li, C. Liang, R. Yu, and S. Liu, "AMC-loaded wideband base station antenna for indoor access point in MIMO system," *IEEE Transactions on Antennas and Propagation*, vol. 63, no. 2, pp. 525–533, 2015.

[11] S. Rajagopal, G. Chennakesavan, D. R. P. Subburaj, R. Srinivasan, and A. Varadhan, "A dual polarized antenna on a novel broadband multilayer artificial magnetic conductor backed surface for LTE/CDMA/GSM base station applications," *AEU-International Journal of Electronics and Communications*, vol. 80, pp. 73–79, 2017.

[12] S. Sarkar and B. Gupta, "A dual-band circularly polarized antenna with a dual-band AMC reflector for RFID readers," *IEEE Antennas and Wireless Propagation Letters*, vol. 19, no. 5, pp. 796–800, 2020.

[13] J.-N. Lee, K.-C. Lee, and P.-J. Song, "The design of a dual-polarized small base station antenna with high isolation having a metallic cube," *IEEE Transactions on Antennas and Propagation*, vol. 63, no. 2, pp. 791–795, 2015.

[14] S. Khan, H. Ali, M. Khalily et al., "Miniaturization of dielectric resonator antenna by using artificial magnetic conductor surface," *IEEE Access*, vol. 8, pp. 68548–68558, 2020.

[15] S. X. Son Xuat Ta and I. Ikmo Park, "Dual-band low-profile crossed asymmetric dipole antenna on dual-band AMC surface," *IEEE Antennas and Wireless Propagation Letters*, vol. 13, pp. 587–590, 2014.

[16] M. Ameen, O. Ahmad, and R. K. Chaudhary, "Wideband circularly-polarised high-gain diversity antenna loaded with metasurface reflector for small satellite applications," *Electronics Letters*, vol. 55, no. 15, pp. 829–831, 2019.

[17] A. P. Volkov, V. V. Kakshin, I. Y. Ryzhov, K. V. Kozlov, and A. Y. Grinev, "Wideband low-profile dual-polarized antenna with AMC reflector," *Progress in Electromagnetics Research Letters*, vol. 88, pp. 15–20, 2020.

[18] Q. Liu, H. Liu, W. He, and S. He, "A low-profile dual-band dual-polarized antenna with an AMC reflector for 5G communications," *IEEE Access*, vol. 8, pp. 24072–24080, 2020.